

Maximum Independent Set Problem in King's Lattice of Order Three via QuEra Architecture

Team Atomique: David, Dmitrii, Kevin, Paarth, Quinn

February 4, 2024

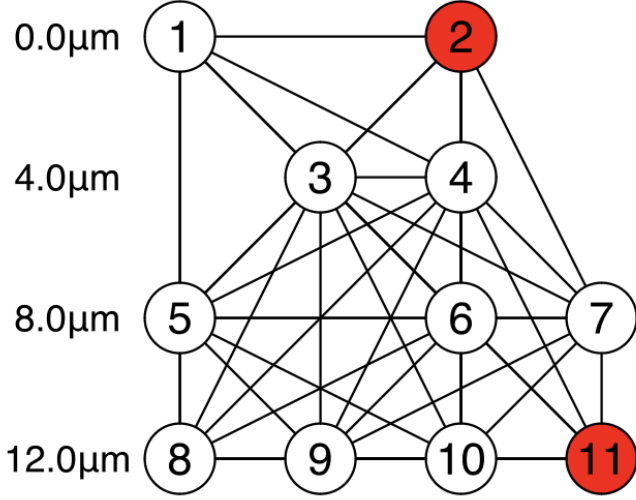


Figure 1: An example King's lattice graph with order $12\mu\text{m}$. The vertices highlighted in red depict a classically found solution to $|\text{MIS}|$ using Julia's Generic Tensor Network.

1 Introduction

For a given graph with n vertices and m edges, an independent set is a subset of vertices for which no pair of vertices in the subset is connected by an edge. If we maximize the size of such a set, we consider this a solution to the Maximum Independent Set (MIS) problem: $|\text{MIS}|$.

Solutions to MIS have been realized by utilizing a two-dimensional Rydberg atom array. A good approximation for the Hamiltonian governing a system of Rydberg atoms is (ignoring phase):

$$H = \sum_n \Omega(t)[|r\rangle_n \langle g|_n + h.c.] - \sum_j \Delta_j(t)n_j + \sum_{i,j} \frac{C}{r_b^6} n_i n_j$$

Here, the Hamiltonian prevents two atoms within a radius $r_b = (C_6/\sqrt{(2\Omega)^2 + \Delta^2})^{1/6}$ from simultaneously inhabiting the same state. In our context, we can leverage this behavior to punish the system for being in a non-independent configuration.

To specify our problem further, we only take graphs which are a King's lattice of order $3k$ where k is the unit length of the lattice. This means that for vertices which lie within a disc of radius $3k$ centered at a fixed vertex, edges may be formed between those vertices. To maximize the probability that we

find an $|\text{MIS}|$ using a Rydberg array, our first question then becomes: what value of the blockade radius r_b maximizes the Rydberg interaction strength between connected vertices and minimizes the Rydberg interaction strength between disconnected vertices? To answer this, we turn to geometry.

In Fig. 1, an example of a King's lattice which fits our order parameters is shown. For an order $3k$, we aim to find a blockade radius which extends at least $3k$ away from a center vertex, but at most $\sqrt{10}k$ away. This can easily be seen using Pythagorean theorem, where the nearest neighbor outside the disc of radius $3k$ is at a distance $\sqrt{3^2 + 1^2}k = \sqrt{10}k$. Thus, we fix $3k < r_b < \sqrt{10}k$. To initially fix r_b as a constant for the purposes of straightforward classical emulation, we choose the geometric mean, $r_b = \sqrt{3\sqrt{10}}$.

2 Emulation and Approximate Hamiltonian

In emulations and on real hardware, we take $\Omega \rightarrow 0$ before the in situ image is projected on the Rydberg array. Thus, we can fix a constant maximum value of Δ to obtain our desired value of r_b . If we let Ω go to zero, we find $\Delta = C/r_b^6$.

The trouble is a balancing act between pushing the states into $|r\rangle$ with a high Rabi frequency Ω , but not too high so as to dominate the van der Waals and detuning terms of the Hamiltonian. Ω must also not be too low, as no Rydberg states will be achieved at all (see Fig. 2).

To find an optimal protocol to run on our emulators and hardware, we thought primarily about tweaking Ω , $\Omega(t)$ pulse wave shape, and $\Delta(t)$ pulse wave shape. The given initial $\Omega(t)$ pulse shape was a trapezoid and $\Delta(t)$ an increasing linear shape, as shown in the Fig. 3. Additionally, to go beyond these given parameters, we also simulated Hamiltonian evolution on QuTIP to get a better grasp on the space of ideal values (see Hamiltonian QuTIP Simulation section).

3 Hamiltonian QuTIP Simulation

To obtain a deeper understanding of the behavior of a Rydberg blockade, especially with regards to the different parameters of distance, detuning, and Rabi frequency, we performed QuTIP simulations.

Setting our r_b to the value described in the introduction, we lock our detuning value δ , since we have our rabi frequency, Ω set to 0 at the end of the procedure.

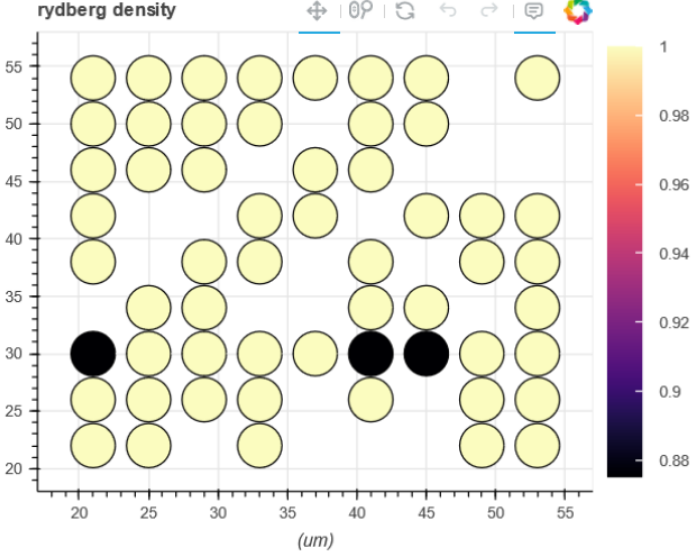


Figure 2: For a zero Ω pulse, the atoms are likely in the ground state as there exists no drive. Note: here, a Rydberg density of 1 corresponds to certainty of finding the atom in the ground state.

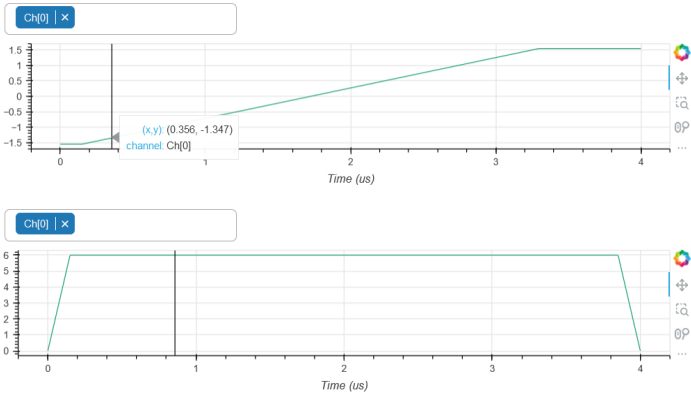


Figure 3: For y-axis frequency and x-axis time (μ s): (top) Example pulse shape of $\Delta(t)$. (bottom) Example trapezoid pulse shape of $\Omega(t)$.

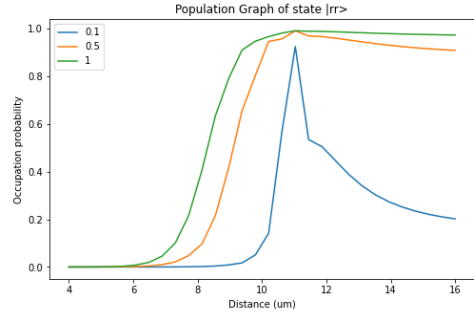


Figure 4: QuTIP simulation of Rydberg blockade as a function of distance

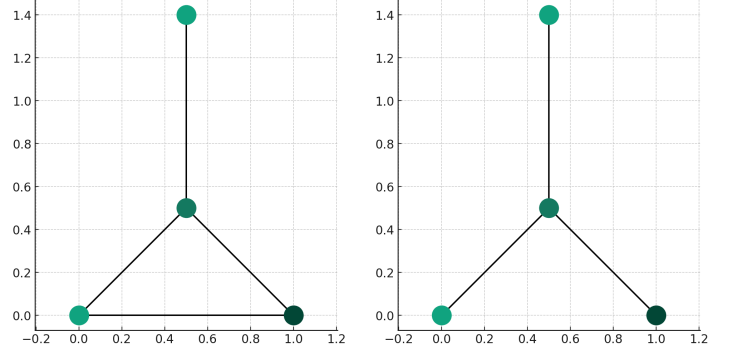


Figure 5: Graphs for annealing vs. VQE comparison

We then simulate the Hamiltonian in the introduction for a simple 2 atom case. We measure the probability that two adjacent atoms enter a Rydberg state and obtain figure 5. From the graph, we see for small distances, the probability of both atoms being excited is very small, but blow up as we exit the Rydberg blockade. The one exception is for when our rabi frequency is set to 0.5, (which is actually $(0.5 * 2\pi)$), where the rabi frequency is too small to force both sites to be populated at the same time (the blue line). We use this to serve as intuition for when we choose our parameters for large scale Rydberg atom arrays.

4 Circuit Representation vs. Blockade

The natural step for us was to compare the annealing solution with the VQE approach. For this task, two similar graphs of four vertices were chosen (see Fig. 2)

From the Rydberg blockade perspective, the graph on the left requires the larger Rydberg radius, R_b , to allow for the connection of the lowest two vertices. Using $R_b = (\frac{C_6}{\Delta})^{1/6}$, we will be able to find the detuning.

For the circuit-based approach, we were explored the ground state of a Hamiltonian defined as

$$H = - \sum_n n_i + U \sum_{i < j} n_i n_j$$

, the ground state of which is guaranteed to represent a MIS. Constant U was chosen to be $\gg 1$ as suggested in (2306.13123). The quantum circuit ansatz is given in figure 6.

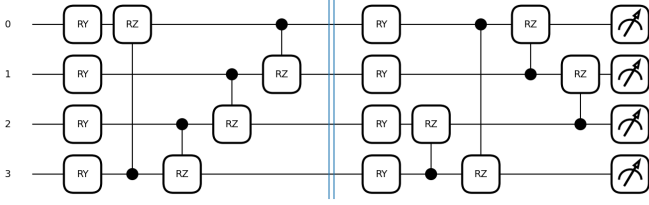


Figure 6: VQE quantum circuit

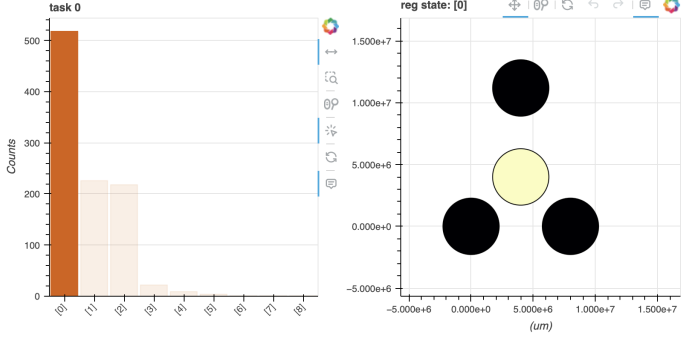


Figure 7: Performance of the annealing model in Bloqade emulation

Throughout the training process in PennyLane, sixteen rotation angles were learned, so the resultant state vector represents the ground state of H .

Performance In summary, both: Bloqade emulation and a simulation on Aquila performed significantly better than the circuit model. Rydberg blockade allowed us to quickly obtain the right solution for both graph, while the quantum circuit took 30 minuts to train and generated correct solutions with lower probabilities. The results for emulation and hardware run for the annealing model on the second graph with $\Delta = 4 \times 2\pi\text{MHz}$ are shown in 7 and 8, respectively.

It can be easily seen that the Rydberg (dark) atoms correspond to MIS for the second graph.

5 Rydberg Atom Array

Fig. 1 depicts a graph solved for $|\text{MIS}|$ by Bloqade’s emulator. We found this solution for a $\Omega = 6\text{MHz}$ and given initial pulse shapes. When reproduced on real hardware, however, our solution fell apart (see Fig. 9). This demonstrated that parameters which solved for $|\text{MIS}|$ on the emulator, do not always hold on hardware. (Some emulations of simpler graphs

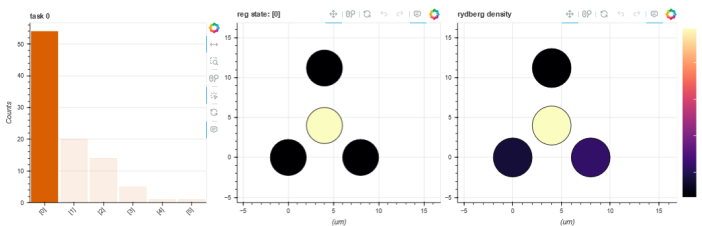


Figure 8: Performance of the annealing model on Aquila

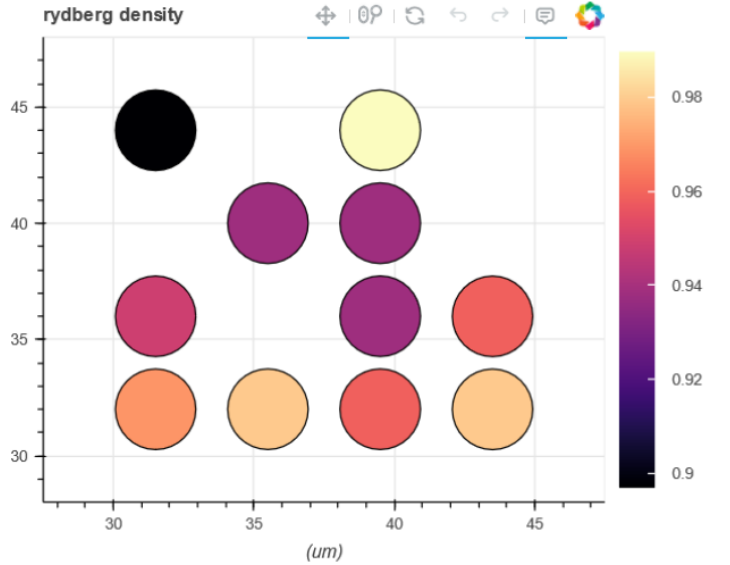


Figure 9: The 4 by 4 graph depicted in Fig. 1, but solved on hardware. The graph here is a heatmap of the Rydberg densities per each vertex (or atom).

actually do predict solutions obtained on hardware very well. See the Circuit Representation vs. Blockade section.)

We wrote a function which quantifies the probability of obtaining independent sets from real hardware with a given set of parameters. It returns the ratio of total independent sets measured in a 100 shot task to the number of measured output states. We call this the Independent Set Ratio (ISR). For the 4 by 4 graph, this value was 0.212. When we expand to a 9 by 9 graph, however, we get very few independent sets (one of which is shown in Fig. 10). The ISR for this graph was 0.0548.

This low ISR suggests that parameters need to be re-optimized for the 9 by 9 graph. We noticed most of our outcome states were dominated by ground states. We attempted to increase the slope of the increasing linear $\Delta(t)$ which would “reward” states for jumping to $|r\rangle$ (as the Hamiltonian goes as $-\Delta$ not $+\Delta$) earlier in the pulse duration.

This of course risks varying the Δ parameter too fast which might push us into a non-adiabatic domain. In the end, this re-optimization did not yield better results for the 9 by 9 graph.

6 Applications

Heat Distribution in 3D Integrated Circuits: The relentless pursuit of Moore’s Law, aiming for the doubling of transistors on integrated circuits (ICs) approximately every two years, has propelled the semiconductor industry into the era of three-dimensional Integrated Circuits (3D ICs). Unlike traditional 2D ICs where components are spread across a single plane, 3D ICs stack multiple layers of silicon wafers or dies, interconnected by through-silicon vias (TSVs). This architectural evolution offers significant advantages, including reduced footprint, lower power consumption, and the potential for higher performance due to shorter interconnect distances.

However, this leap in design complexity introduces a

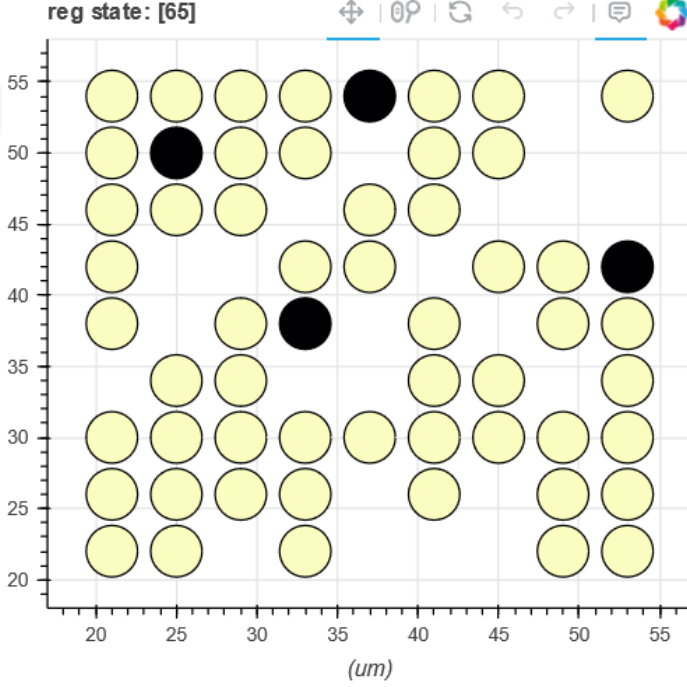


Figure 10: An independent set of size 4 obtained on hardware from a 9 by 9 graph.

formidable challenge: thermal management. The vertical stacking of active layers significantly increases power density, exacerbating heat accumulation within the device. Heat dissipation in 3D ICs is hindered by the limited surface area available for heat exchange compared to the internal volume where heat is generated[1].

Graph theory provides a powerful framework for modeling complex systems, including the thermal behavior of 3D ICs. By representing heat sources (such as CPU cores, memory blocks, and other power-generating components) as nodes and their thermal interactions as edges, we can abstract the 3D IC's thermal profile into a graph model. This abstraction enables the application of mathematical and computational techniques to analyze and optimize the system.

Our approach of using Maximum Independent Set aims to distribute heat sources across the IC in a manner that facilitates uniform heat dissipation and reduces the likelihood of hot spot formation.

To quantify heat transfer within a 3D IC, we employ Fourier's law of heat conduction, which describes the rate of heat flow Q through a material:

$$Q = -kA \frac{dT}{dx}$$

where: Q is the heat flow rate (in watts, W), k is the thermal conductivity of the material (in watts per meter-kelvin, W/mK), A is the cross-sectional area perpendicular to the heat flow direction (in square meters, m²), $\frac{dT}{dx}$ is the temperature gradient in the direction of heat flow (in kelvin per meter, K/m).

For discrete components in a 3D IC, the heat equation can be adapted to:

Complex 2D Graph Representation of a 3D IC Layer for Autonomous Driving

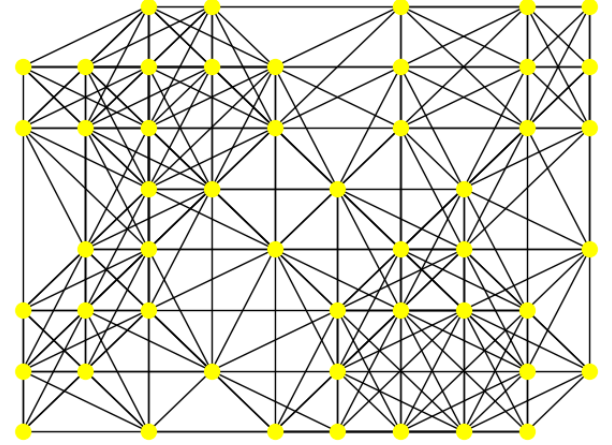


Figure 11: Applications

$$P_i = \sum_{j \in N(i)} \frac{T_i - T_j}{R_{ij}}$$

where P_i is the power dissipation of the i th component, $N(i)$ denotes the set of neighboring components, T_i and T_j are the temperatures of components i and j , respectively, and R_{ij} is the thermal resistance between components i and j .

The process of applying MIS for thermal optimization in 3D ICs involves:

1. **Graph Construction:** Develop a graph model of the 3D IC, mapping components to nodes and thermal interactions to edges.
2. **MIS Identification:** Employ computational algorithms to identify the MIS of the graph, indicating an arrangement of components that minimizes thermal crossover.
3. **Thermal Simulation:** Utilize computational fluid dynamics (CFD) and finite element analysis (FEA) tools to simulate the thermal performance of the 3D IC based on the MIS-guided component placement, validating the effectiveness of the optimization strategy.

In the quest to optimize thermal management within 3D ICs through graph theory, a specific geometric constraint, denoted as $Rb/a = 3$, emerges as a critical factor in guiding the spatial arrangement of heat sources for improved heat distribution. This constraint becomes particularly relevant when applying the Maximum Independent Set concept to achieve an optimal thermal design.

Urban Heat Island Mitigation: Urban Heat Islands (UHI) phenomenon refers to the observed elevated temperatures in urban areas compared to their rural surroundings, primarily due to human activities and modifications of land surfaces. UHIs can exacerbate the energy demand for cooling, contribute to air pollution and greenhouse gas emissions, and negatively impact human health and comfort. Mitigating UHI effects is a critical challenge in urban planning and environmental sustainability.

Graph theory offers a novel lens through which urban planners can address the UHI phenomenon. By conceptualizing

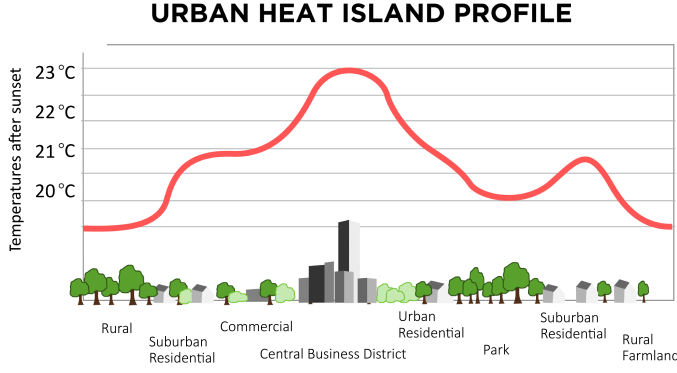


Figure 12: Urban Heat Application

the urban landscape as a graph, with nodes representing areas contributing to UHI (such as buildings, roads, and other impervious surfaces) and edges representing potential paths for heat distribution or mitigation strategies, planners can apply the Maximum Independent Set concept to identify optimal configurations for reducing heat accumulation.

The $Rb/a = 3$ constraint, representing an optimal spatial distribution ratio, can guide the placement of green infrastructure (GI) and other cooling features in the urban graph model. This ratio ensures that interventions are neither too clustered, which could limit their cooling benefits, nor too dispersed, which might reduce their overall effectiveness in mitigating UHI effects.

For practical quantum computing applications in UHI mitigation, the focus is on near-term quantum computers, which operate with an order of a few hundred qubits. Applying the MIS concept within a graph-theoretical framework, augmented by the $Rb/a = 3$ spatial constraint, presents a promising strategy for mitigating the Urban Heat Island phenomenon. This approach allows urban planners to systematically identify and implement the most effective interventions, ensuring that urban designs are both sustainable and conducive to mitigating environmental challenges. Through careful planning and strategic implementation of green infrastructure, cities can become more resilient against the effects of UHIs, leading to healthier, more livable urban environments.

7 Conclusion

Solving the MIS problem for King's lattices of order $3k$ required significant thought about the optimal protocol for a given set of parameters. In all, we believe we put a lot of thought and work into finding optimal parameters, but rushed to a big graph (9 by 9) too fast. We did not put enough thought into our definition of a function which returns the probability of finding an independent set given a graph. A great learning experience!

References

- [1] A. Jain, R. E. Jones, Ritwik Chatterjee, S. Pozder and Zhihong Huang, "Thermal modeling and design of 3D integrated circuits," 2008 11th Intersociety Conference

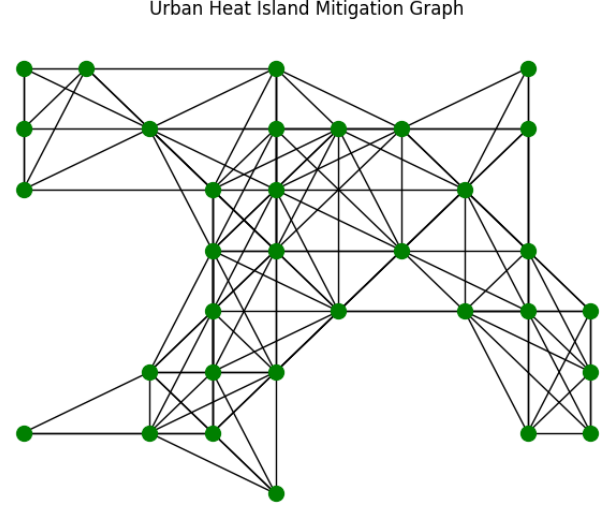


Figure 13: Heat Island Mitigation Graph Example

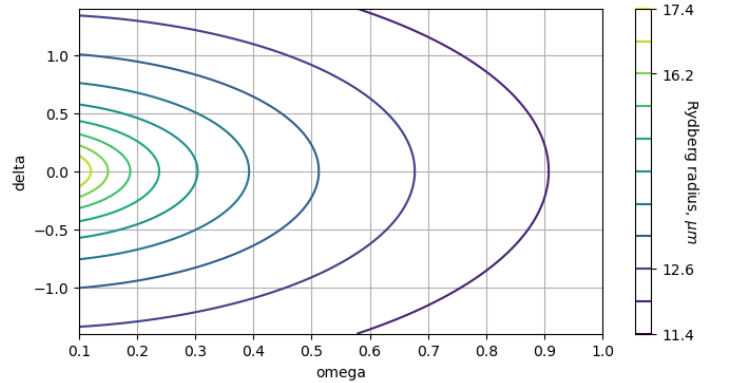


Figure 14: Additional figure noting the space of Ω , Δ parameters around a certain r_b value.

on Thermal and Thermomechanical Phenomena in Electronic Systems, Orlando, FL, 2008, pp. 1139-1145, doi: 10.1109/ITHERM.2008.4544389.